Electronic Supplementary Material (ESI) for CrystEngComm.

Mapping Surface Morphology and Phase Evolution of Iron Sulfide Nanoparticles

Tao Yang,[a] Yurong He,[a,b] Xiaotong Liu,[a,b,c] Xiulei Liu,[a] Qing Peng,*[d, e] Ning Li,[a] Jinjia Liu*[b,c]

[a] *Beijing Advanced Innovation Center for Materials Genome Engineering, Industry-University Cooperation Base between Beijing Information S&T University and Synfuels China Technology Co. Ltd, Beijing, China.*

[b] *State Key Laboratory of Coal Conversion, Institute of Coal Chemistry, Chinese Academy of Sciences, Taiyuan, 030001, P.R. China.*

[c] *National Energy Center for Coal to Clean Fuels, Synfuels China Co., Ltd, Huairou District, Beijing, 101400, P.R. China*

[d] *Physics Department, King Fahd University of Petroleum & Minerals, Dhahran 31261, Saudi Arabia*

[e] *K.A.CARE Energy Research & Innovation Center at Dhahran, Dhahran, 31261, Saudi Arabia*

* Corresponding author:

Jinjia Liu (liujinjia@sxicc.ac.cn)

Qing Peng (qing.peng@kfupm.edu.sa)

Contents

Fig. S4 The contour diagram of sulfur chemical potential (μ_S , eV) versus temperature and gaseous pressure (P_{H2S}/P_{H2}), the rectangle regions represents the sulfur chemical potential under typical experimental preparation conditions.

Fig. S5 The surface energy of FeS-M with different terminations.

Fig. S6 The surface energy of FeS-T with different terminations.

Fig. S7 The surface energy of Fe_9S_{10} with different terminations.

Fig. S8 The surface energy of Fe_7S_8 with different terminations.

Fig. S9 The surface energy of Fe_3S_4 with different terminations.

Fig. S10 The surface energy of FeS_2-P with different terminations.

Fig. S11 The surface energy of FeS_2-M with different terminations.

Fig. S12 The surface energy (γ, J/m^2) of the most stable terminations as a function of sulfur chemical potential (μ_S , eV), a-c for FeS-T, Fe_9S_{10}, and FeS_2-M, respectively.

Fig. S13 The morphology of Fe nanoparticles with different sizes.

Fig. S14 The morphology of different size FeS-M nanoparticles under varying temperatures.

Fig. S15 The morphology of different size FeS-T nanoparticles under varying temperatures.

Fig. S16 The morphology of different size Fe_9S_{10} nanoparticles under varying temperatures.

Fig. S17 The morphology of different size Fe_7S_8 nanoparticles under varying temperatures.

Fig. S18 The morphology of different size Fe_3S_4 nanoparticles under varying temperatures.

Fig. S19 The morphology of different size FeS_2-P nanoparticles under varying temperatures.

Fig. S20 The morphology of different size FeS_2-M nanoparticles under varying temperatures.

Table S1 The lattice constant and k mesh used in surface energy calculations.

	hkl	a×b (Å)	K-mesh
FeS-M	(001)	3.59×3.59	6×6×1
	(100)	6.62×3.59	4×6×1
	(110)	5.56×5.07	4×4×1
	(111)	5.07×6.62	4×4×1
	(112)	5.07×7.53	4×3×1
	(221)	7.53×6.63	3×4×1
FeS-T	(100)	3.33×5.10	6×4×1
	(101)	6.09×3.33	4×6×1
	(102)	7.69×3.33	3×6×1
	(202)	6.09×3.33	4×6×1
Fe_9S_{10}	(100)	6.61×26.70	3×1×1
	(220)	26.70×6.61	1×3×1
	(111)	6.61×27.51	3×1×1
Fe_7S_8	(100)	6.57×15.52	3×2×1
	(110)	15.52×11.38	2×2×1
	(111)	11.38×16.86	2×2×1
	(203)	35.58×6.57	1×3×1
	$(10\bar{2})$	6.57×19.25	3×1×1
	$(20\bar{6})$	6.57×23.31	3×1×1
Fe_3S_4	(001)	6.70×6.70	4×4×1
	(011)	9.48×6.70	3×4×1
	(311)	11.61×6.70	2×4×1
	(111)	6.70×6.70	4×4×1
	(211)	16.42×6.70	2×4×1
	(220)	9.48×6.70	3×4×1
FeS_2-P	(100)	5.40×5.40	4×4×1
	(110)	5.40×7.63	4×3×1
	(111)	7.63×7.63	3×3×1
	(210)	5.40×12.07	4×2×1
	(211)	9.35×7.63	3×3×1
	(230)	5.40×19.46	4×1×1
	(231)	9.35×12.07	3×2×1
	(311)	13.22×7.63	2×3×1
FeS_2-M	(001)	4.44×5.41	5×4×1
	(011)	4.44×6.38	5×4×1
	(020)	3.39×4.44	7×5×1
	$(11\bar{1})$	6.38×5.58	4×5×1
	$(1\bar{2}\bar{1})$	7.77×5.58	3×4×1
	(210)	3.39×11.69	7×2×1
	(211)	7.77×6.38	3×4×1

According to our previous study, PBE + U with U_{eff} = 2.0 eV could give reasonable structural, magnetic and electronic properties for iron sulfides when compared to experimental observations.[1] Here we assess the performance of different functional in predicting the thermodynamic property of iron sulfides. We calculate the thermodynamic formation energy (G_f) of FeS, Fe_7S_8, Fe_3S_4, and FeS_2. These phases are selected since the G_f of these four sulfides are previously reported. In this section, we choose LDA, GGA (PBE and PBE*sol*), DFT + U (U_{eff} = 2.0/2.5 eV) and HSE approach. The calculated results and reference data are presented in **Table S2**. LDA approach underestimates G_f for all these four compounds, whilst PBE approach overestimates the formation energy of these iron sulfides. PBE + U with U_{eff} = 2.0/2.5 eV also overestimates the thermodynamic formation energies of Fe_xS_y, especially for pyrite FeS_2-P. For the HSE approach, the computational G_f is extremely overestimated. The overestimation may ascribe to that the twenty-five percent of Hartree-Fock is excessive to describe the Coulomb correlation at Fe sites. It is worth noting that PBE*sol* could give relatively reasonable predictions on G_f for Fe_xS_y, the maximum absolute error is just 0.05 eV/atom for FeS-M case. Previous work has also proved that PBE*sol* is better at describing properties for iron carbides.[2] Therefore, all calculations in this work are based on PBE*sol* functional.

Table S2 The calculated thermodynamic formation energy (ΔG_f, eV/atom) with different functional at 0 K and the absolute error (AE, eV/atom) compared to experimental values.

	FeS-M		Fe_7S_8		Fe_3S_4		FeS_2-P	
	ΔG_f	AE	ΔG_f	AE	ΔG_f	AE	ΔG_f	AE
LDA	-0.72	-0.06	-0.69	-0.15	-0.61	-0.11	-0.83	-0.14
PBE	-0.52	0.14	-0.39	0.15	-0.39	0.11	-0.50	0.19
PBE*sol*	-0.61	0.05	-0.56	-0.02	-0.49	0.01	-0.72	-0.03
U = 2.0	-0.20	0.46	-0.35	0.19	-0.30	0.20	-0.38	0.31
U = 2.5	-0.11	0.55	-0.42	0.12	-0.50	0.00	-0.35	0.34
HSE06	-0.13	0.53	-0.14	0.40	-0.33	0.17	-0.40	0.29
Ref.	-0.66[3]	-	-0.54[4]	-	-0.50[5]	-	-0.69[6]	-

Table S3 The critical sulfur chemical potential (eV) in different iron sulfide phases.

Fe_xS_y	μ_S^{criti} (eV)
FeS-M	-4.36
FeS-T	-3.95
Fe_9S_{10}	-4.13
Fe_7S_8	-4.18
Fe_3S_4	-4.0
FeS_2-P	-4.23
FeS_2-M	-4.23

Table S4 The contribution (%) of each surface to the total exposed surface area under different sulfur chemical potentials.

Fe_xS_y	(hkl)	μ_S (eV)		
		-3.8	-3.4	-3.0
FeS-M	(001)	16.6	6.8	0.1
	(101)	14.3	15.3	17.1
	(111)	29.8	34.4	42.9
	(112)	39.3	43.5	39.9
FeS-T	(100)	26.6	76.4	52.7
	(101)	0	0	47.3
	(102)	34.8	23.6	0
	(202)	38.6	0	0
Fe_9S_{10}	(100)	3.8	2.6	0
	(110)	32.7	64.9	88.6
	(111)	63.5	32.5	11.4
Fe_7S_8	(100)	3.0	62.4	96.4
	(111)	34.7	0	0
	(203)	0.3	0	0
	($\bar{1}02$)	62.0	37.6	3.6
Fe_3S_4	(001)	4.0	54.1	3.8
	(011)	50.5	41.7	0
	(311)	45.5	4.2	96.2
FeS_2-P	(100)	18.8	0	11.7
	(210)	51.6	70.6	61.8
	(211)	30.0	16.0	3.2
	(311)	0	13.4	23.3
FeS_2-M	(001)	1.1	0	0
	(011)	12.5	36.1	67.8
	(020)	1.1	0	0
	(120)	21.5	19.5	6.8
	($\bar{1}11$)	29.5	12.9	0
	($\bar{1}21$)	0.1	0	0
	(211)	34.2	31.5	25.4

Table S5 The detailed information of Fe nanoparticles with different sizes.

Particle size (nm)	Number of atoms	Surface area ($Å^2$)	Corrected surface energy (kJ/mol)
10	38669	29257.83	446337.4
5	5085	7314.458	111584.4
2	339	1170.312	17853.5

Table S6 The detailed information of different size FeS-M nanoparticles under varying temperatures.

Particle size (nm)	Temperature (K)	Number of atoms	Surface area (Å^2)	Corrected surface energy (kJ/mol)
10	100	30113	31460.37	119191.2
	200	29969	31283.52	121394.2
	300	29969	31088.39	123779.4
	400	29969	30889.97	126161.1
	500	29263	30687.38	128550
	600	29007	30481.74	130936.2
	700	29007	30273.88	133313.3
	800	29007	30064.2	135675.6
	900	29007	29853.59	138017.2
	1000	29637	29642.92	140332.1
5	100	3705	7865.108	29797.85
	200	3705	7820.896	30348.6
	300	3705	7772.102	30944.88
	400	3705	7722.49	31540.25
	500	3543	7671.852	32137.54
	600	3543	7620.438	32734.06
	700	3479	7568.468	33328.31
	800	3479	7516.054	33918.92
	900	3479	7463.418	34504.4
	1000	3775	7410.722	35082.99
2	100	239	1258.416	4767.651
	200	235	1251.341	4855.768
	300	235	1243.536	4951.178
	400	235	1235.597	5046.434
	500	235	1227.495	5142.003
	600	235	1219.273	5237.461
	700	235	1210.954	5332.524
	800	235	1202.57	5427.036
	900	235	1194.145	5520.693
	1000	235	1185.716	5613.284

Table S7 The detailed information of different size FeS-T nanoparticles under varying temperatures.

Particle size (nm)	Temperature (K)	Number of atoms	Surface area (Å^2)	Corrected surface energy (kJ/mol)
10	100	15801	18103.55	42147.15
	200	18277	19204.82	48943.57
	300	20905	20291.93	56524.63
	400	23159	21270.48	64234.07
	500	25805	22146.88	72010.27
	600	27795	22918.38	79712.23
	700	30735	24919.04	92137.6
	800	39395	27958.08	109240.9
	900	46925	31329.36	128600.1
	1000	55783	34675.98	149568.2
5	100	1897	4525.891	10536.8
	200	2221	4801.201	12235.89
	300	2533	5072.982	14131.16
	400	2747	5317.62	16058.51
	500	3083	5536.722	18002.58
	600	3503	5729.6	19928.08
	700	3893	6229.764	23034.42
	800	4685	6989.526	27310.25
	900	5693	7832.352	32150.07
	1000	7081	8669.011	33987.28
2	100	113	724.1418	1685.887
	200	147	768.1938	1957.745
	300	135	811.6788	2260.99
	400	207	850.8204	2569.366
	500	207	885.8736	2880.407
	600	207	916.7358	3188.491
	700	267	996.7632	3685.509
	800	315	1118.326	4369.643
	900	315	1253.178	5144.018
	1000	423	1387.046	5982.761

Table S8 The detailed information of different size Fe_9S_{10} nanoparticles under varying temperatures.

Particle size (nm)	Temperature (K)	Number of atoms	Surface area (Å^2)	Corrected surface energy (kJ/mol)
10	100	42453	44531.13	198378.6
	200	47967	46208.88	215080.2
	300	53151	48014.29	233899.9
	400	53517	49801.16	253404.6
	500	59055	51573.33	273618.3
	600	64527	53315.96	294348.3
	700	69891	55016.85	315393.4
	800	75099	56663.29	336516.7
	900	80097	58240.61	357414.9
	1000	84843	59732.62	377722.7
5	100	5479	11132.82	49594.79
	200	6835	11552.24	53770.08
	300	6835	12003.55	58474.84
	400	6835	12450.31	63351.21
	500	8197	12893.32	68404.55
	600	8197	13328.98	73587.05
	700	9511	13754.22	78848.38
	800	9511	14165.83	84129.24
	900	10729	14560.16	89353.77
	1000	10729	14933.18	94430.91
2	100	343	1781.246	7935.156
	200	343	1848.349	8603.194
	300	487	1920.563	9355.969
	400	565	1992.046	10136.17
	500	565	2062.928	10944.72
	600	565	2132.636	11773.92
	700	565	2200.669	12615.72
	800	565	2266.526	13460.64
	900	763	2329.622	14296.58
	1000	763	2389.305	15108.93

Table S9 The detailed information of different size Fe_7S_8 nanoparticles under varying temperatures.

Particle size (nm)	Temperature (K)	Number of atoms	Surface area (Å^2)	Corrected surface energy (kJ/mol)
10	100	10705	15937.56	41700.86
	200	12731	17390.46	48549.86
	300	14781	19033.38	56703.63
	400	16911	20712.49	65622.97
	500	19615	22298.36	75005.59
	600	21729	23740.65	84125.9
	700	24149	25115.42	92301.11
	800	24996	25751.92	96401.77
	900	25222	25986.91	97277.72
	1000	25101	26133.84	96829.43
5	100	1353	3984.39	10425.21
	200	1614	4347.612	12137.46
	300	1875	4758.336	14175.88
	400	2125	5178.126	16405.75
	500	2433	5574.592	18751.41
	600	2697	5935.147	21031.42
	700	3027	6278.867	23075.32
	800	3100	6437.98	24100.44
	900	3116	6496.727	24319.43
	1000	3126	6533.458	24207.35
2	100	85	637.503	1668.036
	200	93	695.6172	1941.992
	300	113	761.3364	2268.148
	400	124	828.4993	2624.919
	500	158	891.9351	3000.227
	600	179	949.6265	3365.038
	700	197	1004.617	3692.044
	800	203	1030.081	3856.085
	900	199	1039.479	3891.119
	1000	197	1045.349	3873.162

Table S10 The detailed information of different size Fe_3S_4 nanoparticles under varying temperatures.

Particle size (nm)	Temperature (K)	Number of atoms	Surface area (Å^2)	Corrected surface energy (kJ/mol)
10	100	59430	15162.54	58802.14
	200	55398	14555.84	56780.68
	300	51222	13748.3	54152.22
	400	45432	12982.75	51458.87
	500	41176	12221.46	48672.03
	600	41176	11472.42	45837.17
	700	36176	10743.41	42980.92
	800	36488	10763.01	43152.05
	900	31560	10327.64	41465.32
	1000	31032	9815.839	39319.95
5	100	6972	3790.646	14700.58
	200	6972	3638.96	14195.17
	300	5992	3437.067	13538.02
	400	5644	3245.683	12864.69
	500	5644	3055.367	12168.01
	600	5644	2868.108	11459.3
	700	4400	2685.852	10745.23
	800	4400	2690.753	10788.01
	900	4400	2581.914	10366.35
	1000	4256	2453.961	9829.992
2	100	448	606.5022	2352.089
	200	448	582.233	2271.226
	300	448	549.9313	2166.084
	400	448	519.31	2058.354
	500	448	488.8589	1946.882
	600	448	458.898	1833.491
	700	448	429.7368	1719.238
	800	364	430.5205	1726.082
	900	180	413.1043	1658.609
	1000	180	392.6336	1572.798

Table S11 The detailed information of different size FeS_2-P nanoparticles under varying temperatures.

Particle size (nm)	Temperature (K)	Number of atoms	Surface area (Å^2)	Corrected surface energy (kJ/mol)
10	100	16965	18932.78	164811.8
	200	24617	24140.16	188819.4
	300	24923	24493.13	194457.8
	400	25523	24853.73	200338.9
	500	26461	25224.29	206511.9
	600	27067	25549.05	212880.4
	700	27259	25865.36	219290.7
	800	27697	26174.74	225668.9
	900	28669	26475.77	231924.5
	1000	28981	26767.13	237957.4
5	100	2137	4733.191	41202.91
	200	3069	6035.064	47205
	300	3129	6123.281	48614.47
	400	3213	6213.439	50084.79
	500	3285	6306.067	51627.93
	600	3291	6387.261	53220.12
	700	3417	6466.363	54822.85
	800	3423	6543.692	56417.25
	900	3603	6618.944	57981.14
	1000	3615	6691.773	59489.29
2	100	131	757.3102	6592.457
	200	203	965.6086	7552.794
	300	203	979.7278	7778.327
	400	203	994.151	8013.573
	500	211	1008.972	8260.487
	600	211	1021.963	8515.233
	700	229	1034.618	8771.662
	800	235	1046.99	9026.757
	900	235	1059.029	9276.966
	1000	235	1070.68	9518.246

Table S12 The detailed information of different size FeS_2-M nanoparticles under varying temperatures.

Particle size (nm)	Temperature (K)	Number of atoms	Surface area (Å^2)	Corrected surface energy (kJ/mol)
10	100	14953	17974.57	119726.9
	200	15489	18650.1	127383.9
	300	16999	19410.64	136086.8
	400	18083	20202.72	145234.7
	500	19265	21033.05	154906.7
	600	20255	21901.24	165098.5
	700	21883	22807.98	175816.7
	800	23147	23754.38	187071.1
	900	24873	24740.94	198861.1
	1000	25845	25764.8	211177.5
5	100	1923	4493.648	29931.76
	200	1965	4662.525	31845.98
	300	2113	4852.648	34021.62
	400	2245	5050.683	36308.71
	500	2329	5258.256	38726.63
	600	2497	5475.32	41274.71
	700	2633	5701.964	43953.92
	800	2921	5938.604	46767.85
	900	3149	6185.228	49715.23
	1000	3255	6441.186	52794.24
2	100	131	718.9829	4789.074
	200	131	746.0028	5095.347
	300	143	776.4248	5443.468
	400	143	808.1076	5809.383
	500	165	841.322	6196.268
	600	167	876.0496	6603.94
	700	179	912.3176	7032.654
	800	205	950.1748	7482.841
	900	213	989.6348	7954.422
	1000	213	1030.594	8447.112

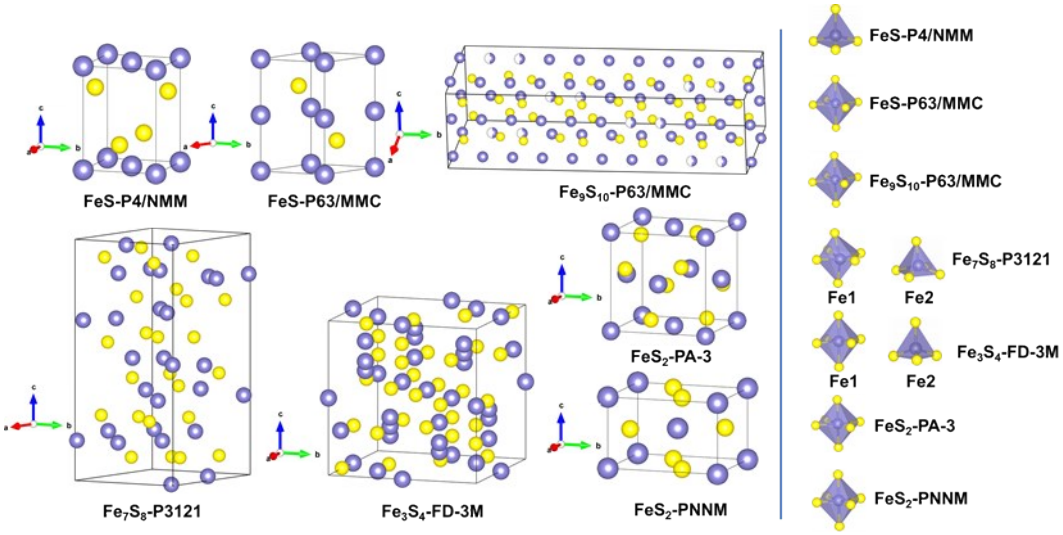

Fig. S1 Left: the crystal structures of iron sulfides; Right: the coordination environment of iron atoms in iron sulfides (blue and yellow spheres represent iron and sulfur atoms, respectively).

The main contribution of temperature on Gibbs free energy (*G*) for solid materials is derived from lattice vibration, namely, the phonon effect. According to our phonon calculations, as shown in **Fig. S2**, one can find that at low temperature, the phonon has a positive effect on *G*, in other words, the phonon effect makes these iron sulfides unstable. However, with the increasing of temperature, the contribution of phonon effect makes iron sulfides more stable in thermodynamic.

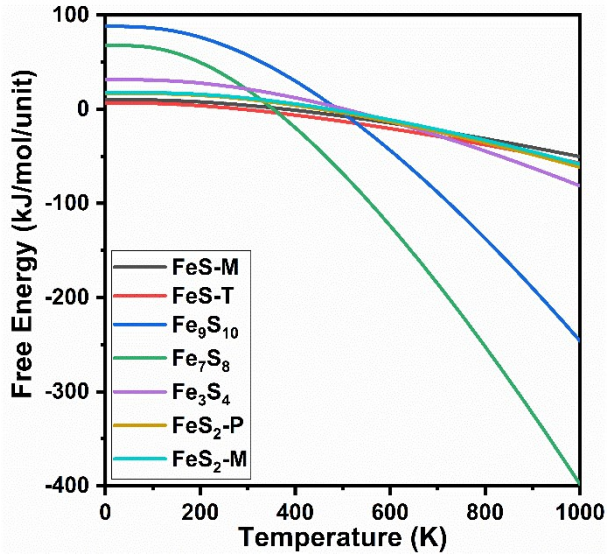

Fig. S2 The phonon contribution to the Gibbs free energy (kJ/mol/unit) of Fe_xS_y as a function of temperature (K).

The reaction free energy (ΔG) from per unit iron to seven iron sulfide phases as a function of μ_S is plotted in **Fig. S3**. In general, with the μ_S increasing, the ΔG is lowered, suggesting that the formation of sulfide is more facile under high external chemical potential. For the bulk phase (**Fig. S3**a), the ΔG from Fe to two polymorph FeS_2 is very close and much lower than other reactions, indicating that the formation of FeS_2 phases is thermodynamically more favourable. For 10 nm particles (**Fig. S3**b), the ΔG of Fe → FeS_2 is slightly rising compared with the bulk phase, but still lower than the ΔG of other transformations. Meanwhile, the formation of FeS-M and Fe_7S_8 is more exothermal relative to the bulk phase.

As for 5 nm nanoparticles (**Fig. S3**c), the ΔG of FeS_2-P formation is slightly lower than that of FeS_2-M phase. When μ_S is around -3.78 eV, the ΔG of Fe to FeS-M and to FeS_2-P is almost the same, demonstrating that under current conditions, the iron could be sulfurized to mixed phases of FeS-M and FeS_2-P. With the particle size of 2 nm, as presented in **Fig. S3**d, when the μ_S is lower than -3.65 eV, the ΔG of FeS-M and Fe_3S_4 formation is very close. When -3.65 < μ_S < -3.26 eV, the formation of Fe_3S_4 is more facile than other phases. However, if μ_S > -3.26 eV, the ΔG of Fe → FeS_2-P is the lowest.

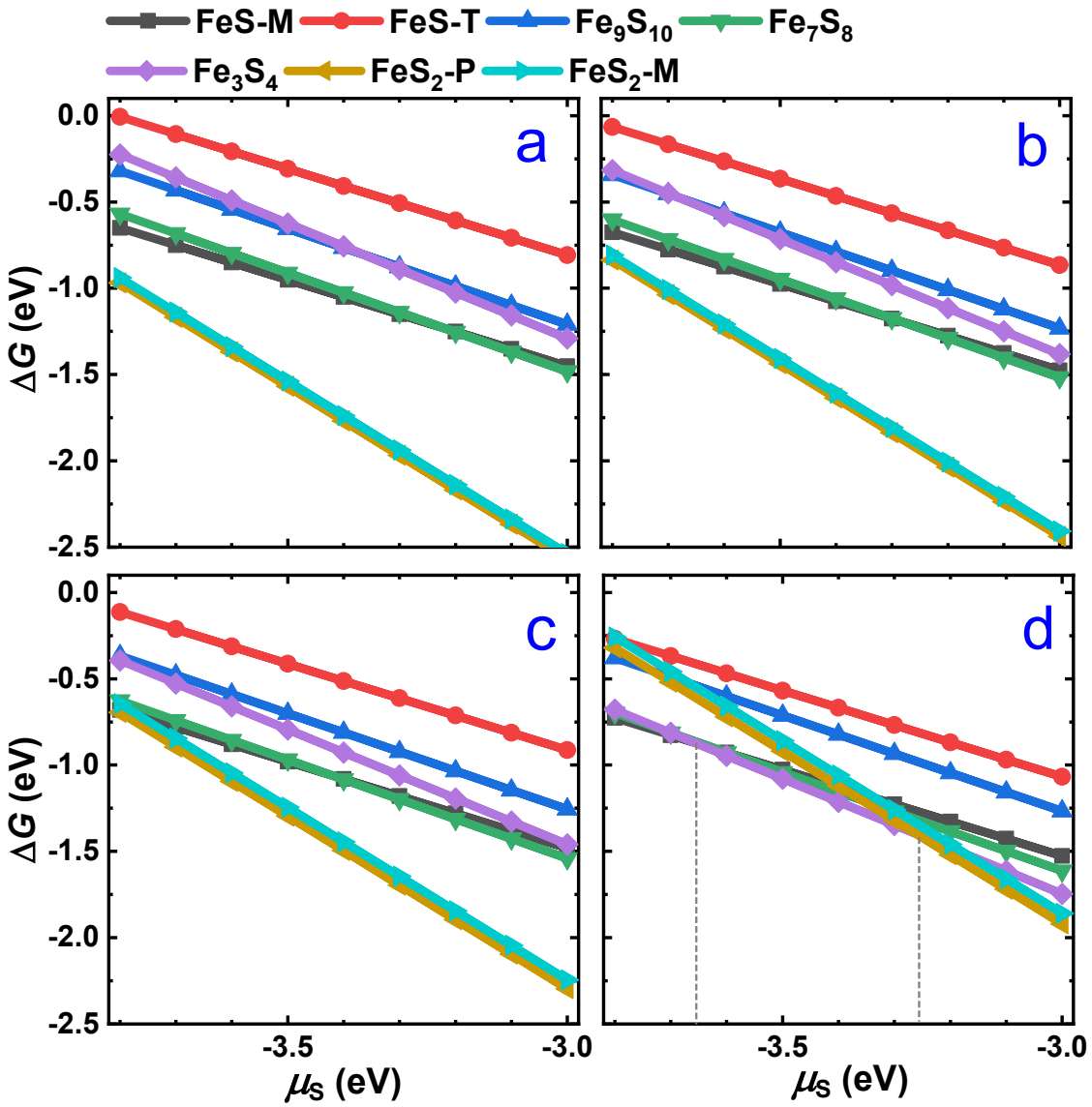

Fig. S3 The reaction free energy (ΔG, eV) of per unit iron to sulfides as a function of sulfur chemical potential (μ_S , eV) at 700 K, **a** for bulk phase, **b** for 10 nm, **c** for 5 nm, and **d** for 2 nm.

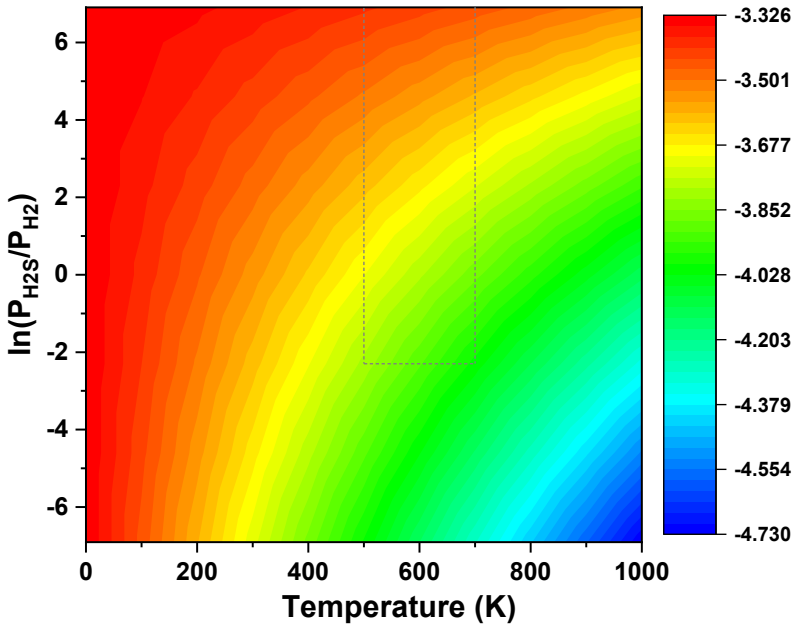

Fig. S4 The contour diagram of sulfur chemical potential (μ_S , eV) versus temperature and gaseous pressure (P_{H2S}/P_{H2}), the rectangle regions represents the sulfur chemical potential under typical experimental preparation conditions.

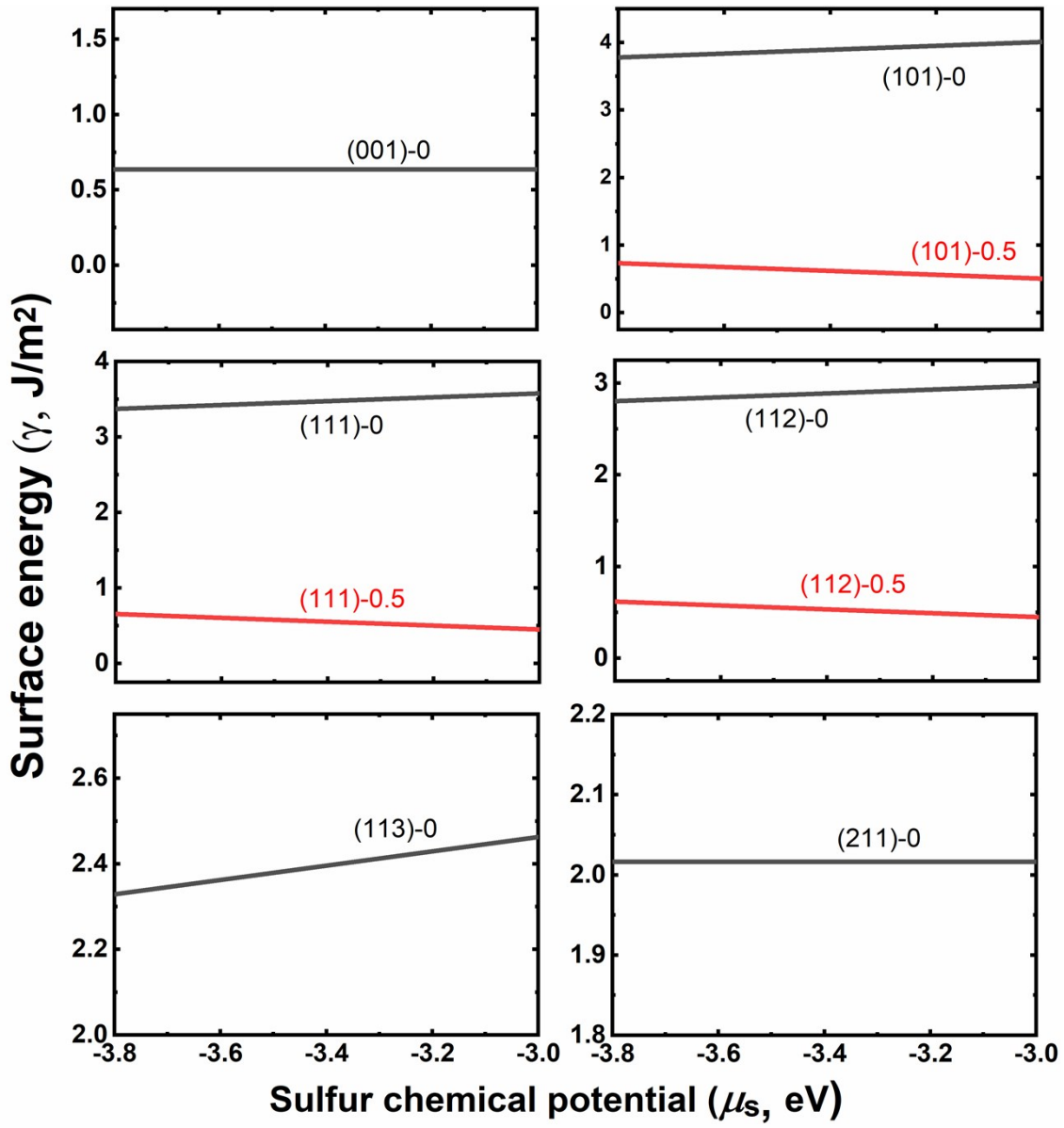

Fig. S5 The surface energy of FeS-M with different terminations.

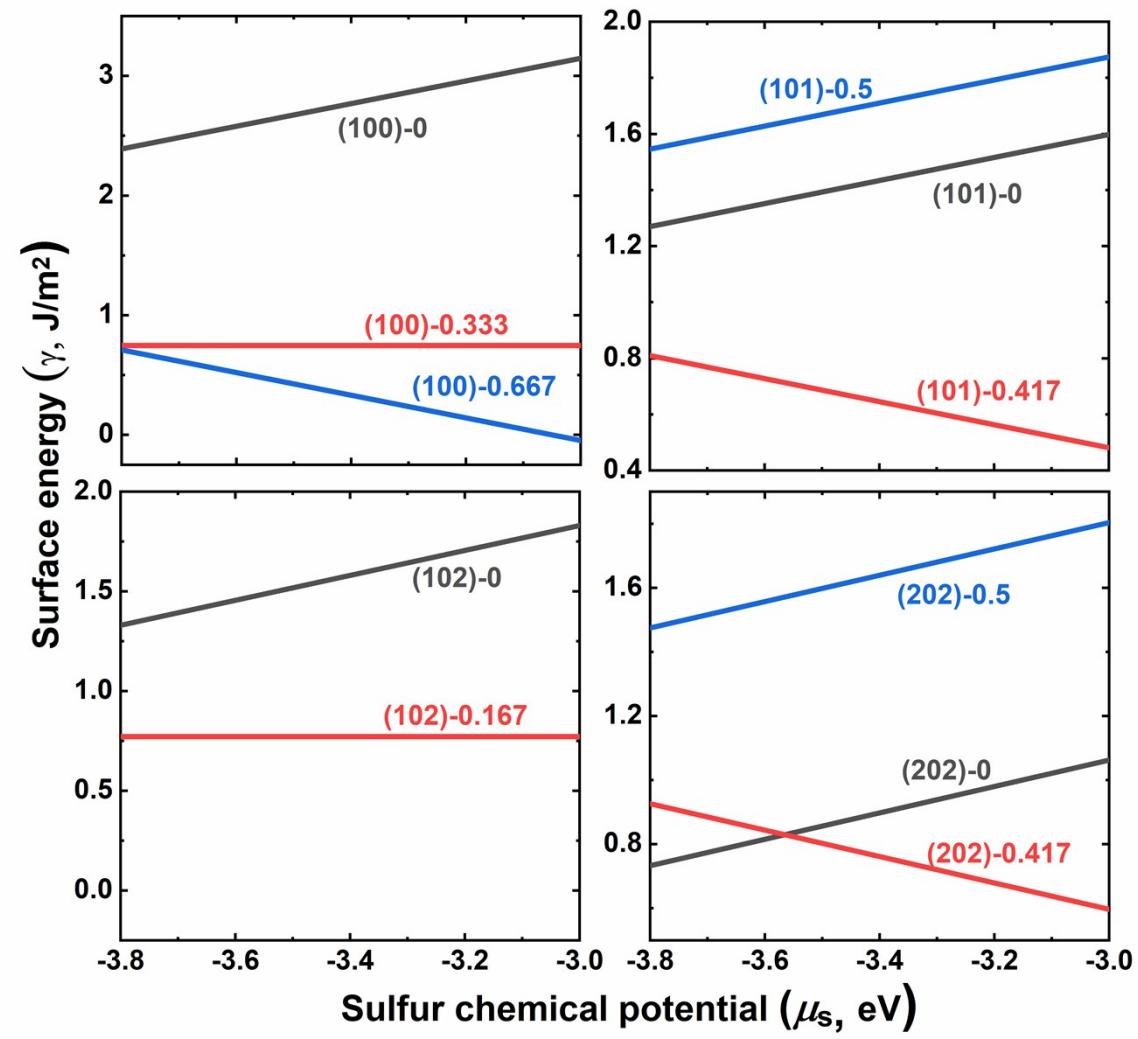

Fig. S6 The surface energy of FeS-T with different terminations.

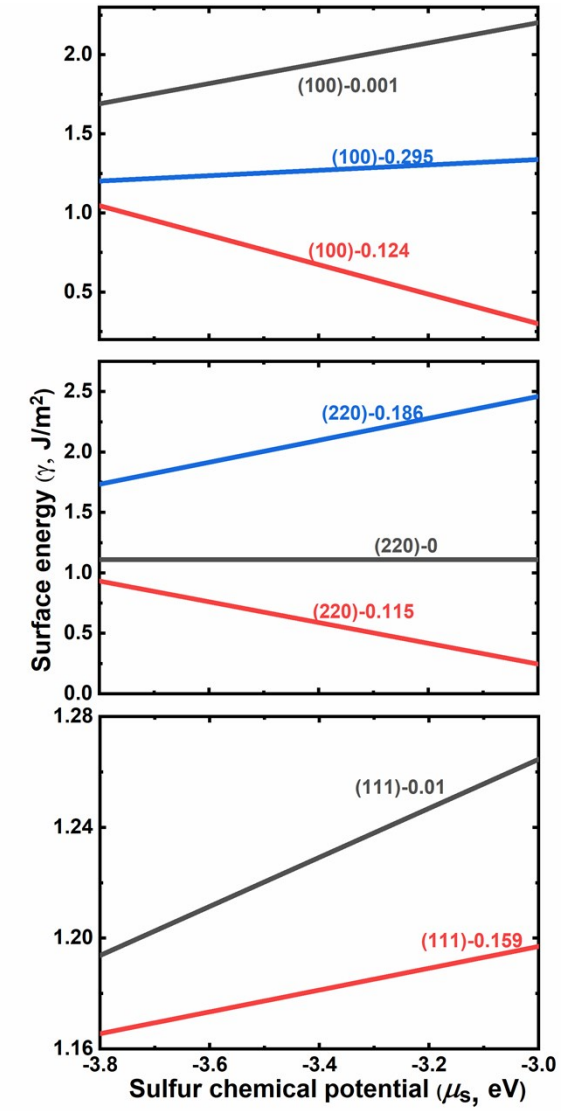

Fig. S7 The surface energy of Fe_9S_{10} with different terminations.

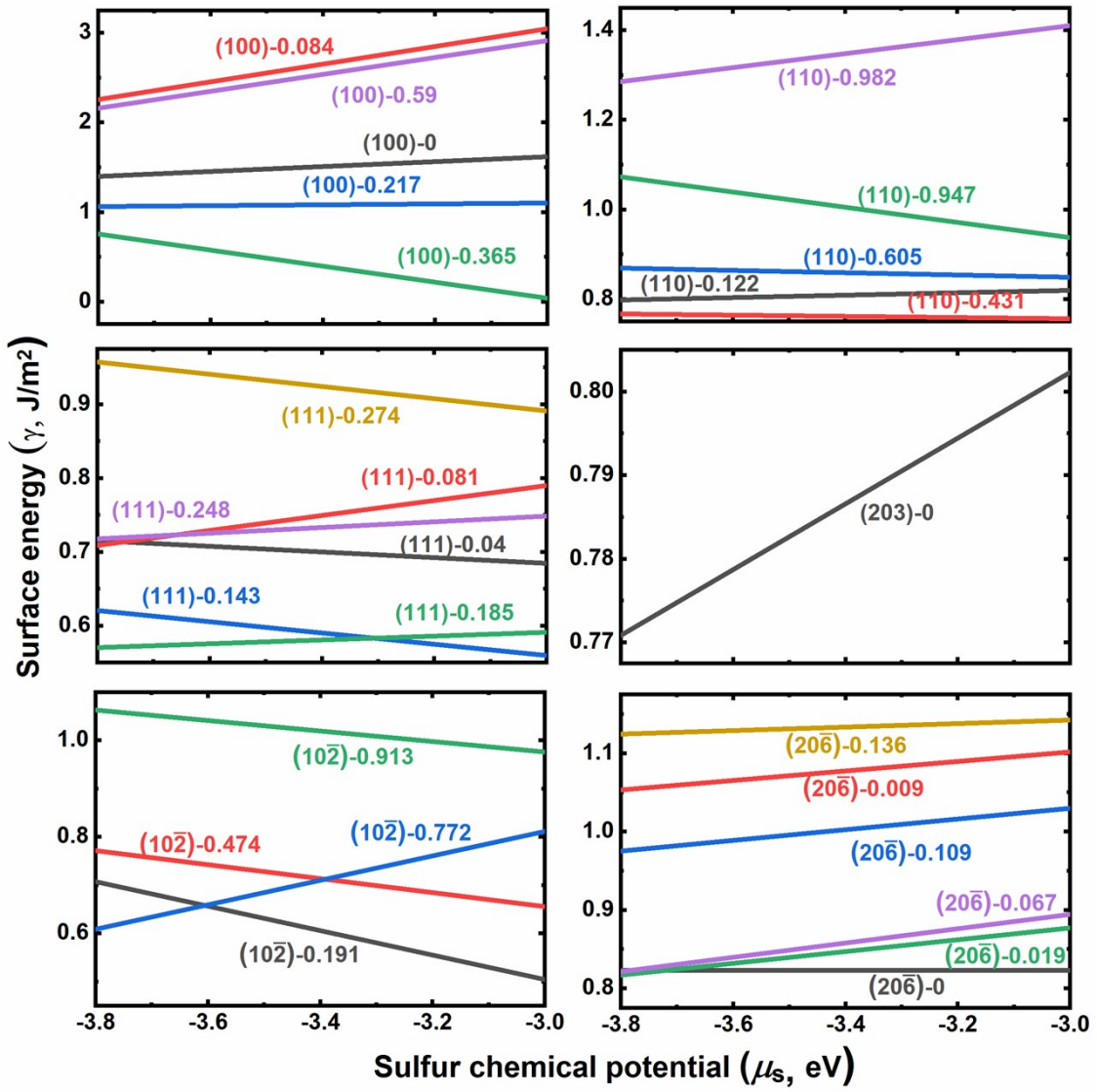

Fig. S8 The surface energy of Fe_7S_8 with different terminations.

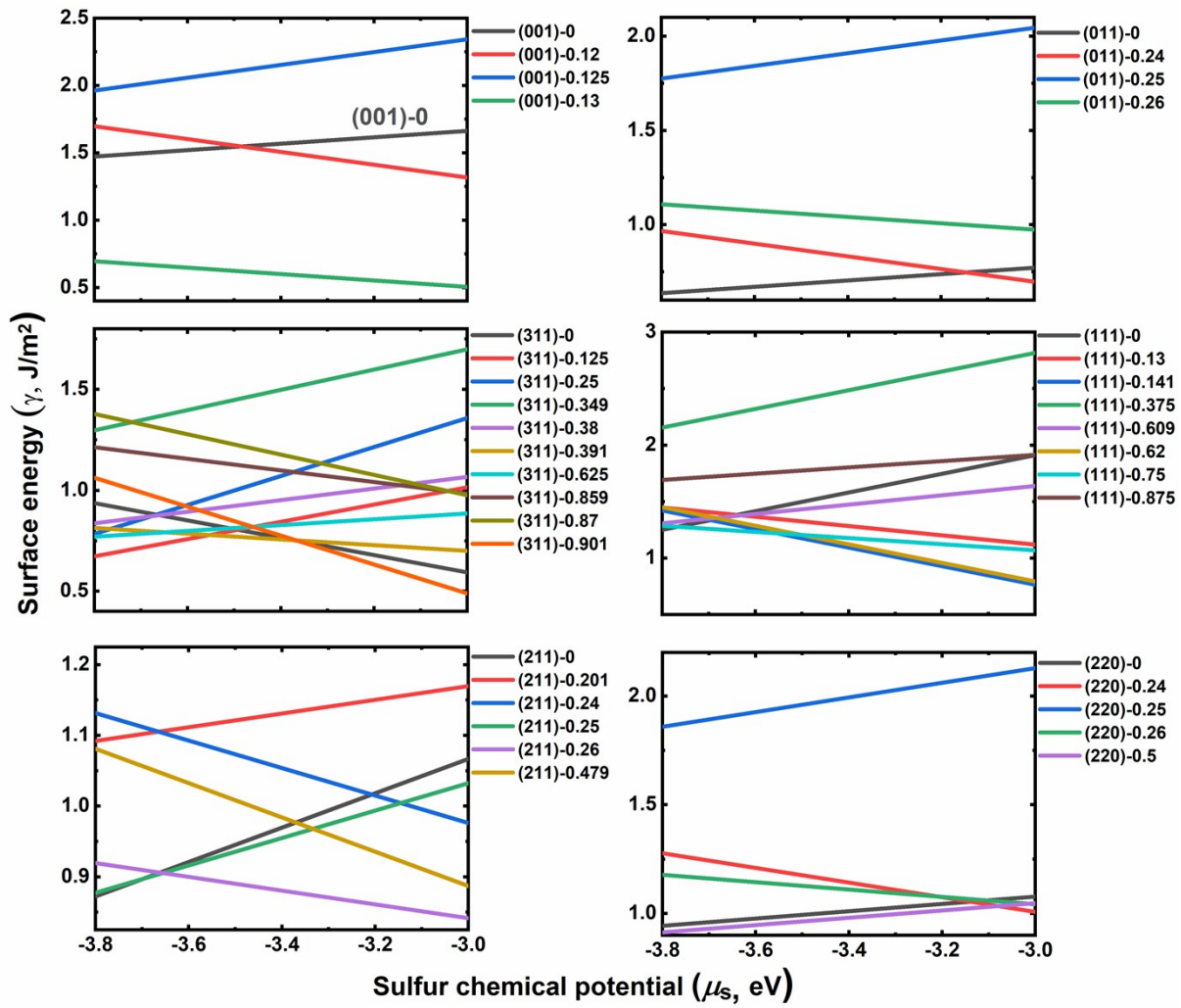

Fig. S9 The surface energy of Fe_3S_4 with different terminations.

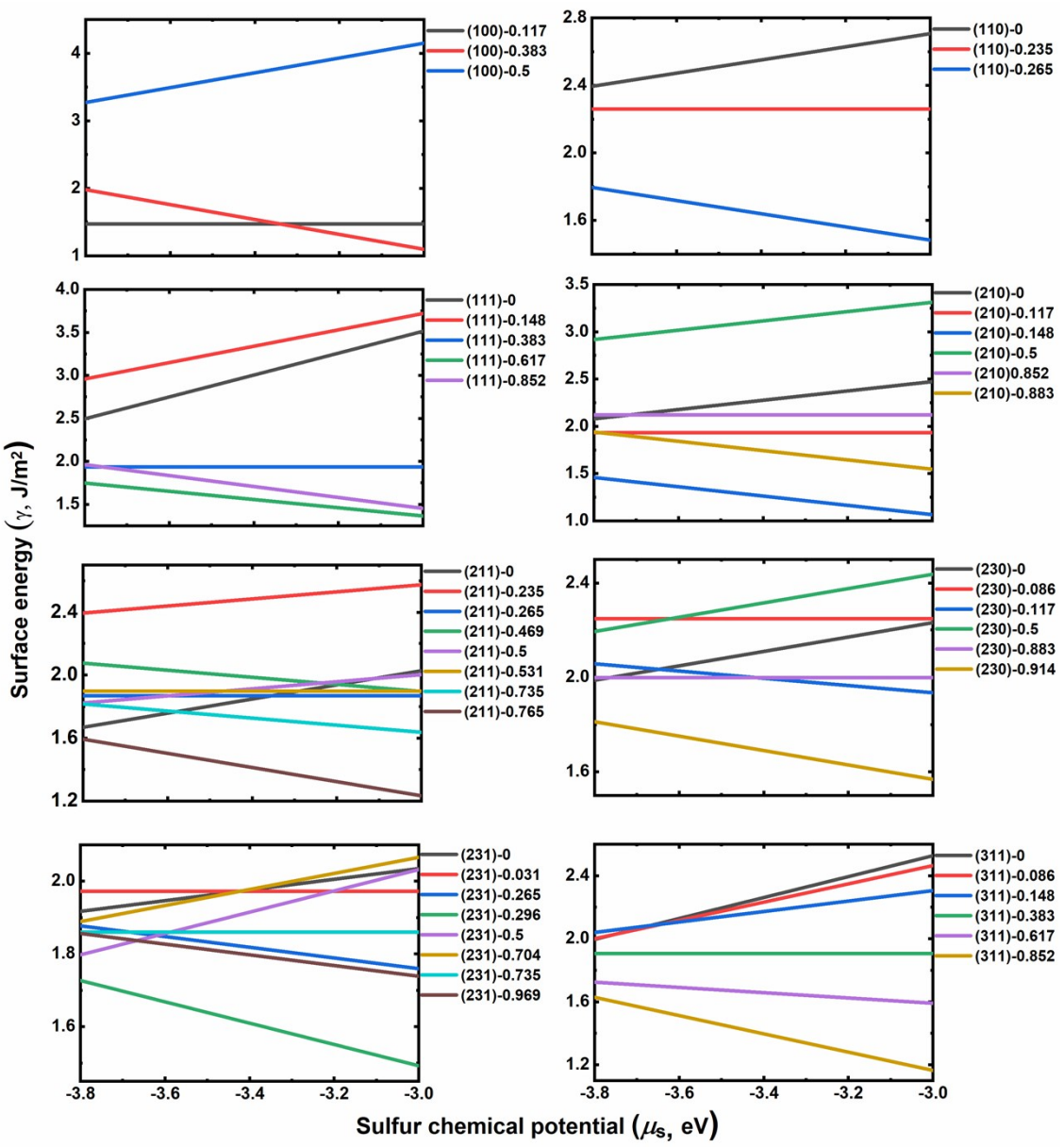

Fig. S10 The surface energy of FeS_2-P with different terminations.

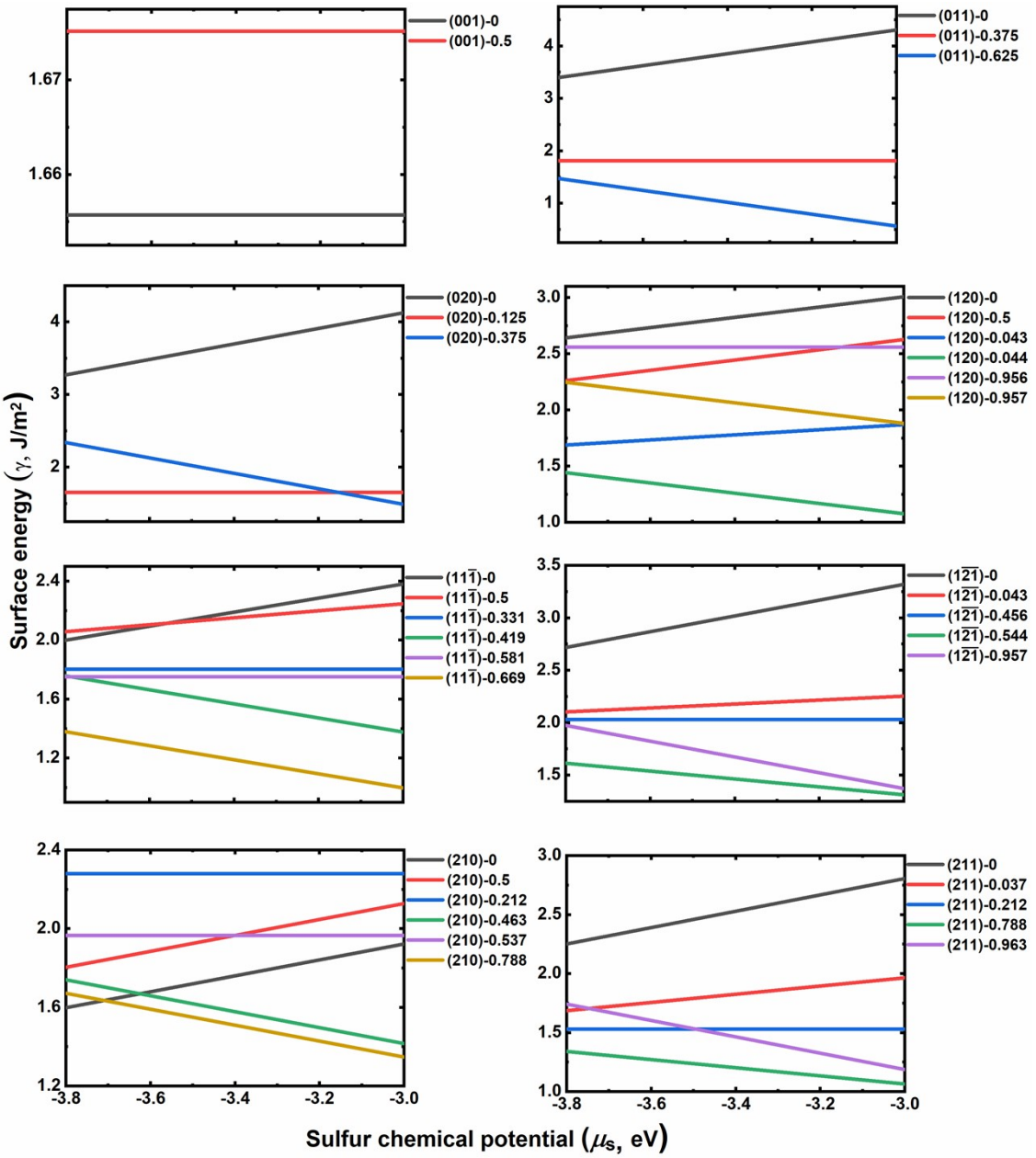

Fig. S11 The surface energy of FeS_2-M with different terminations.

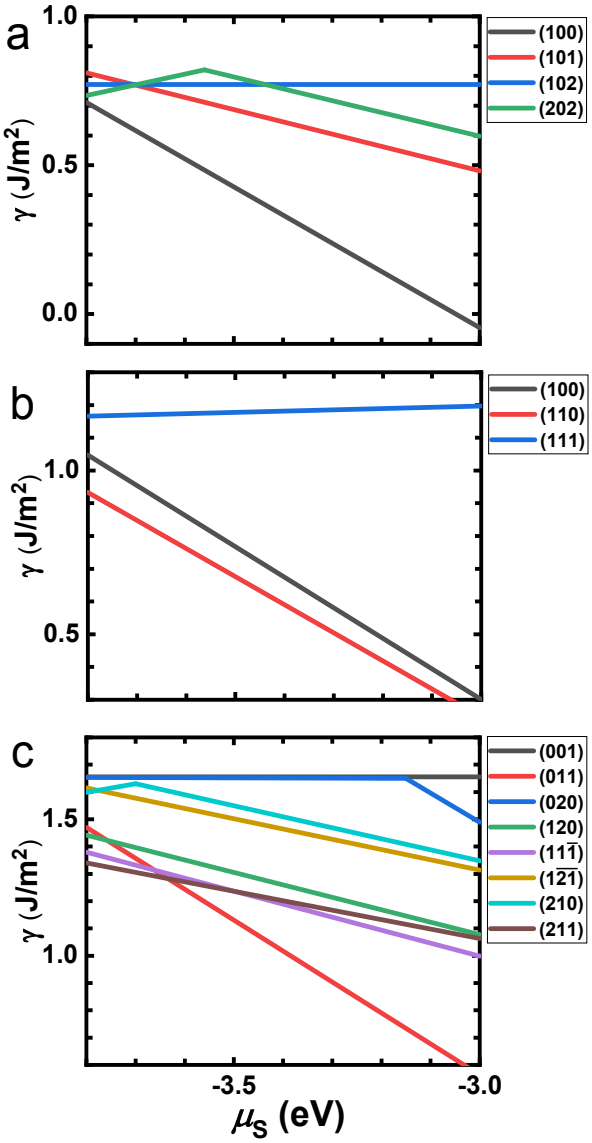

Fig. S12 The surface energy (γ, J/m^2) of the most stable terminations as a function of sulfur chemical potential (μ_S , eV), **a-c** for FeS-T, Fe_9S_{10}, and FeS_2-M, respectively.

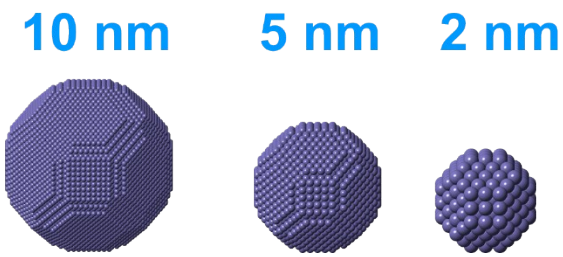

Fig. S13 The morphology of Fe nanoparticles with different sizes.

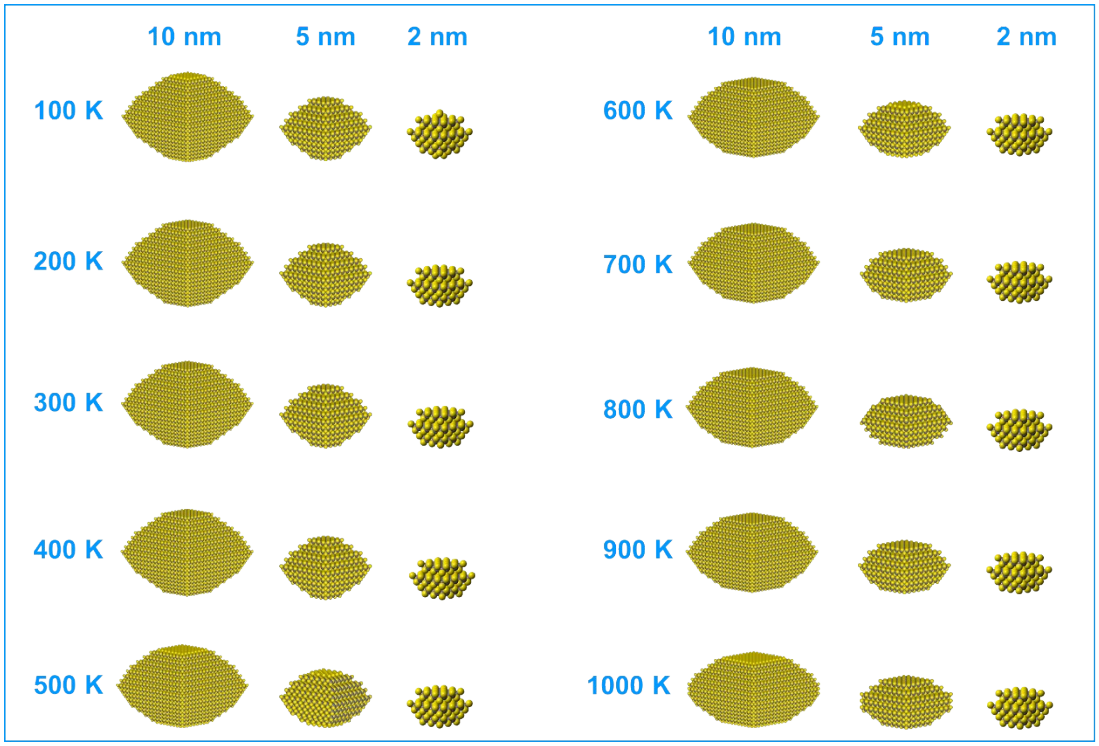

Fig. S14 The morphology of different size FeS-M nanoparticles under varying temperatures.

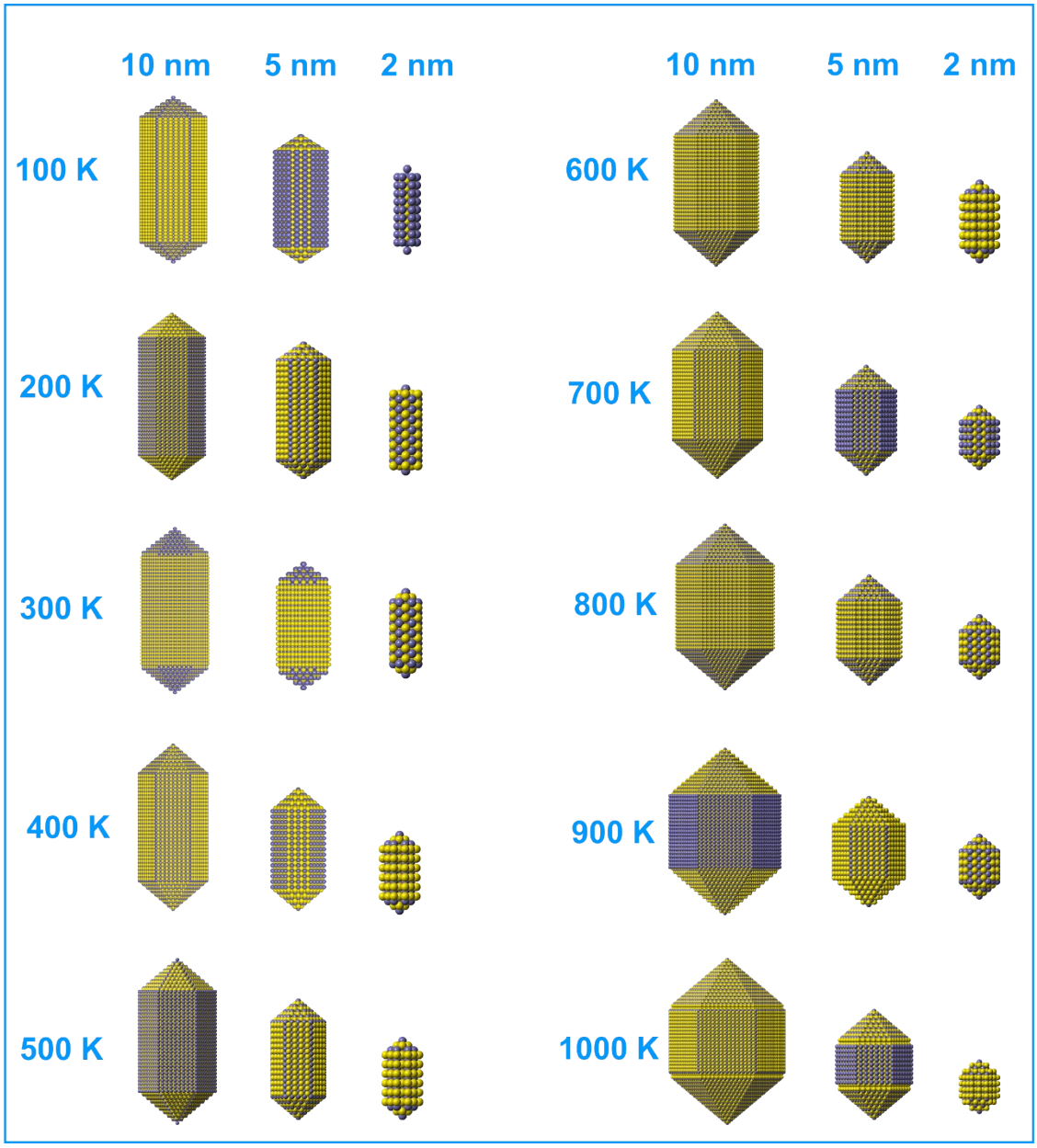

Fig. S15 The morphology of different size FeS-T nanoparticles under varying temperatures.

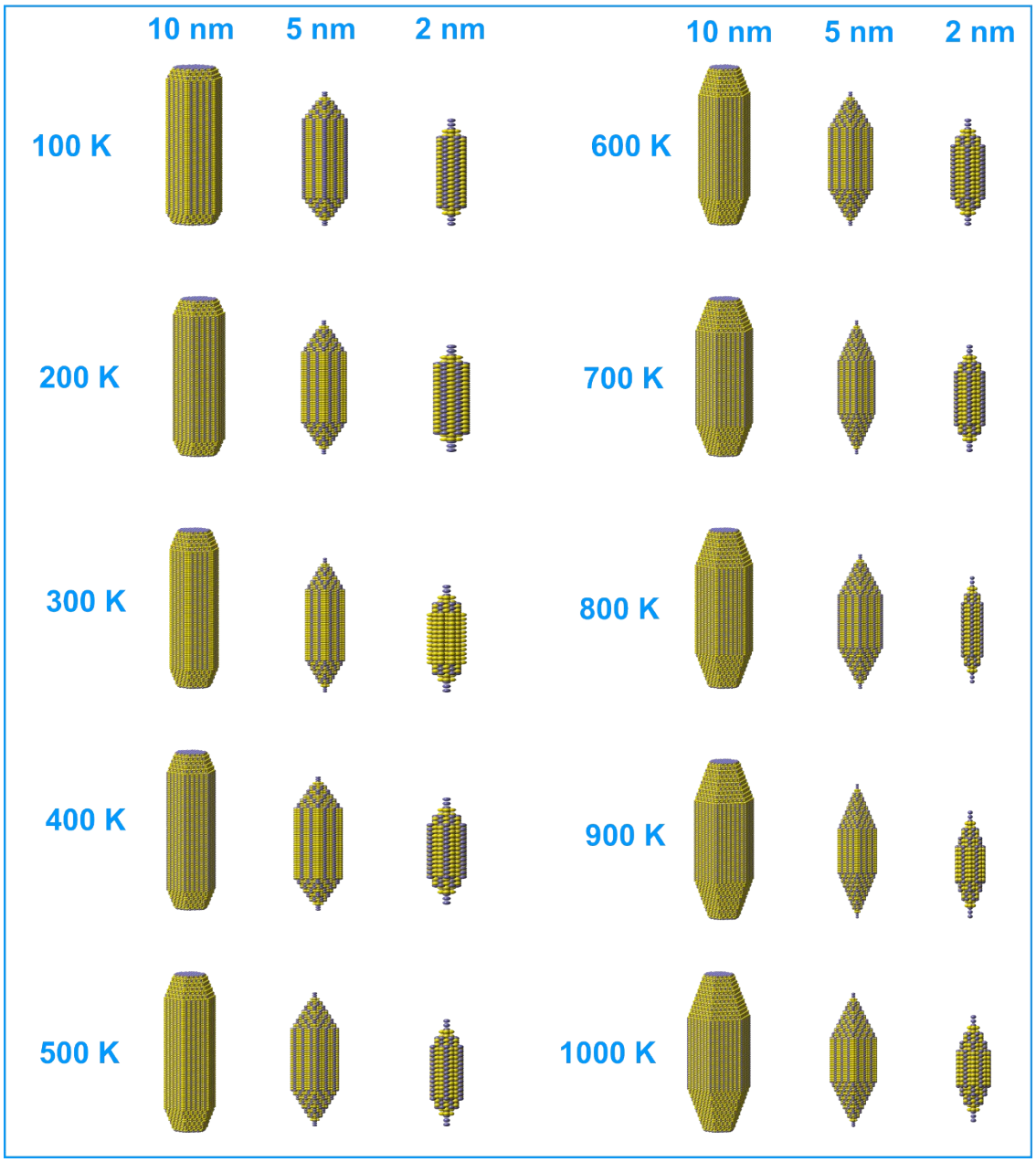

Fig. S16 The morphology of different size Fe_9S_{10} nanoparticles under varying temperatures.

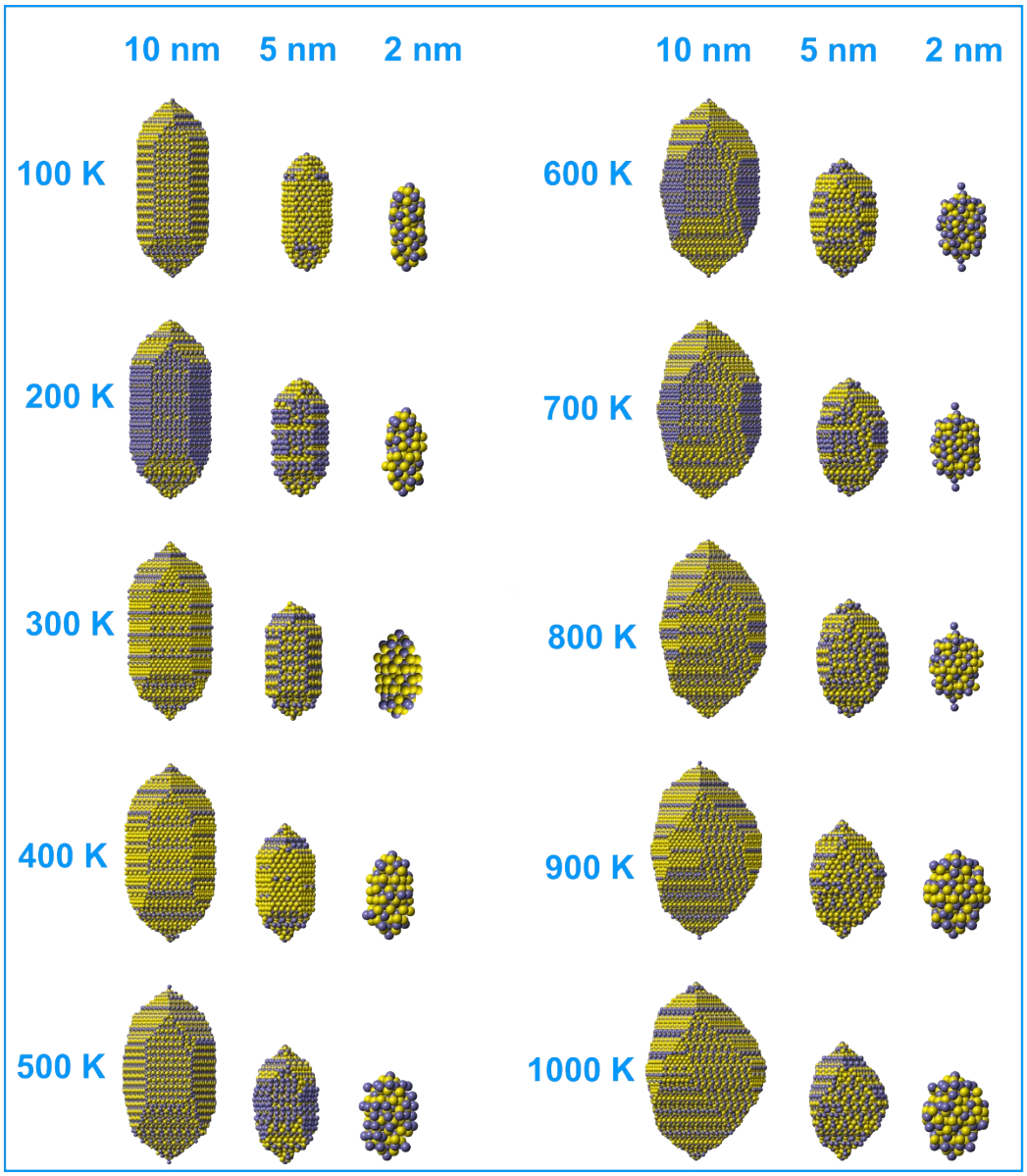

Fig. S17 The morphology of different size Fe_7S_8 nanoparticles under varying temperatures.

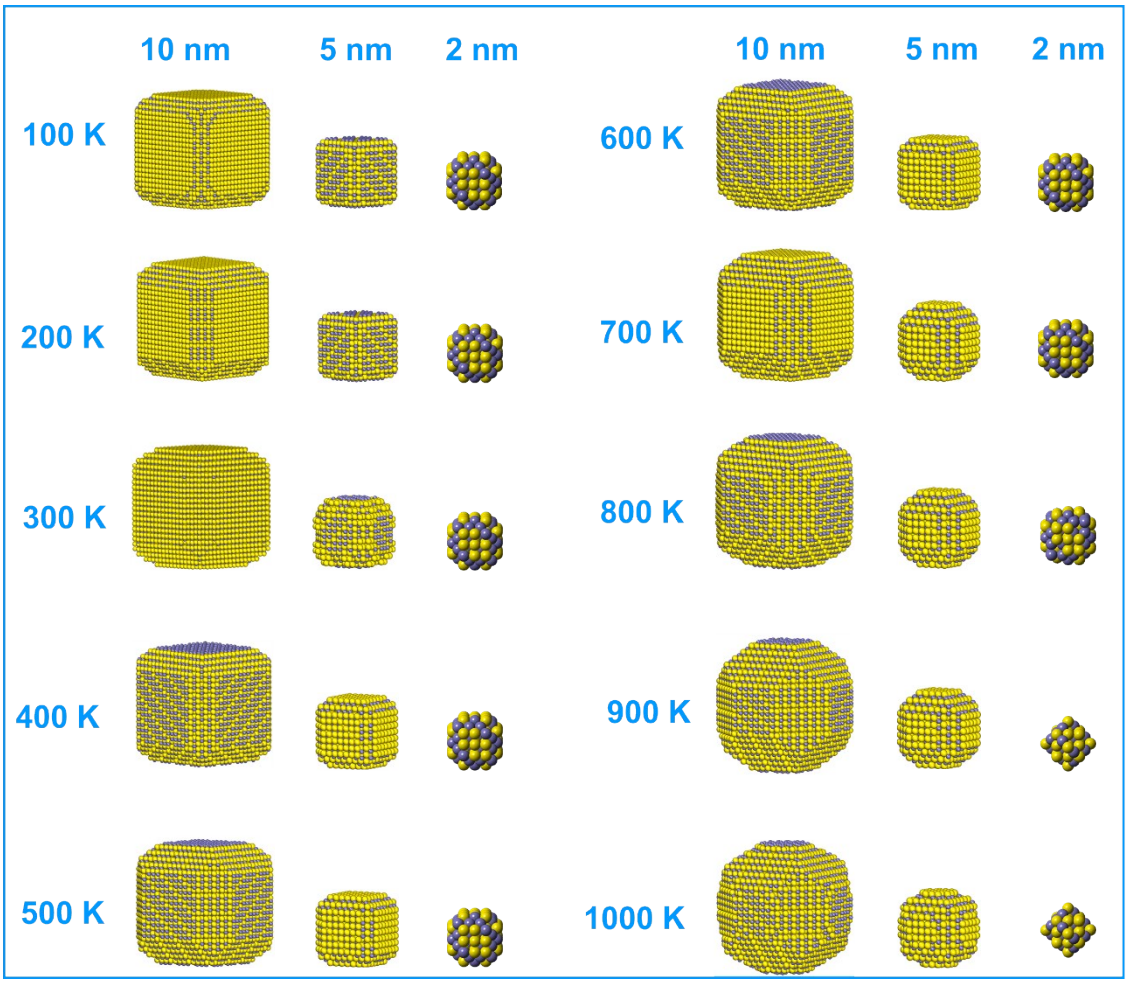

Fig. S18 The morphology of different size Fe_3S_4 nanoparticles under varying temperatures.

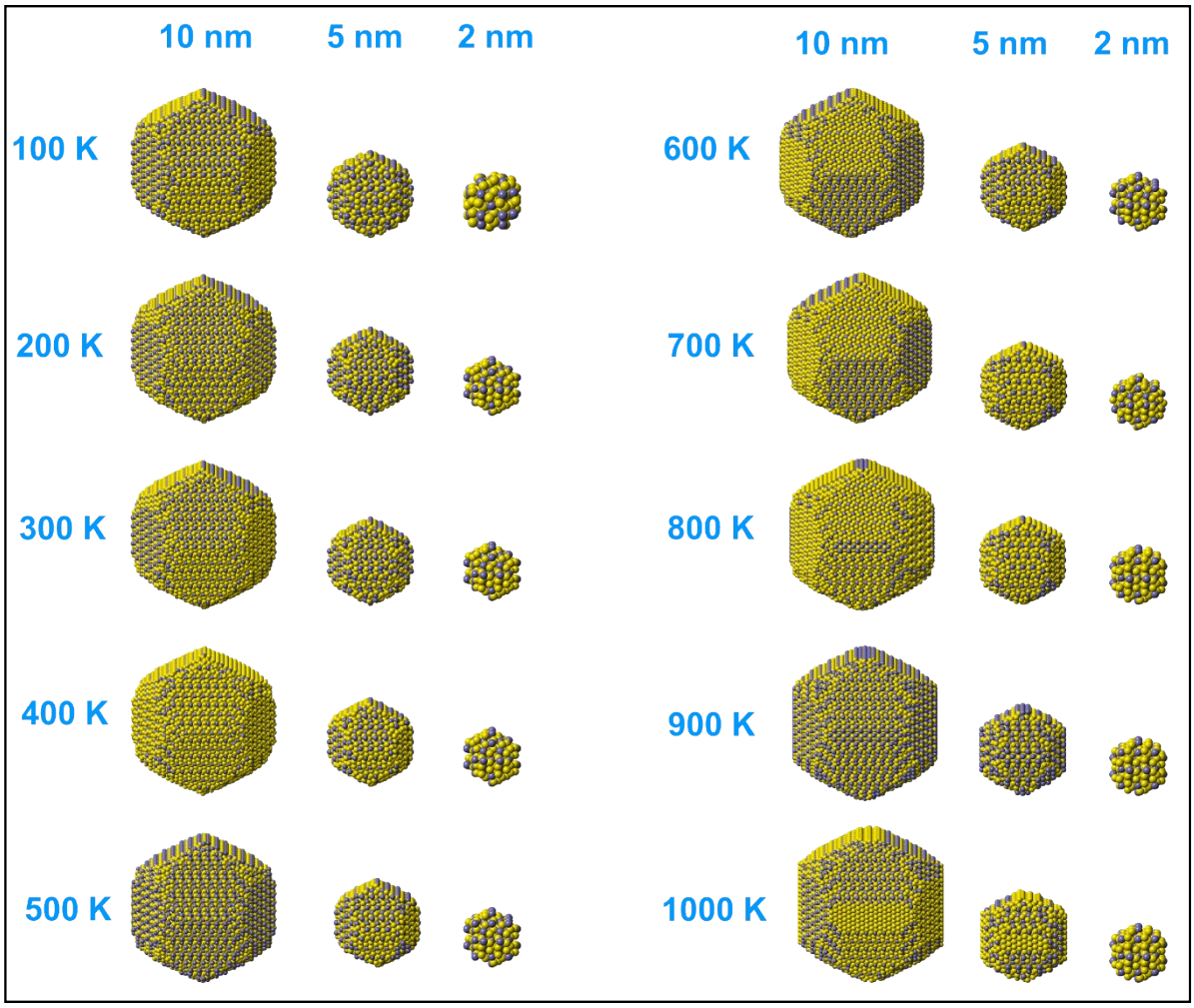

Fig. S19 The morphology of different size FeS_2-P nanoparticles under varying temperatures.

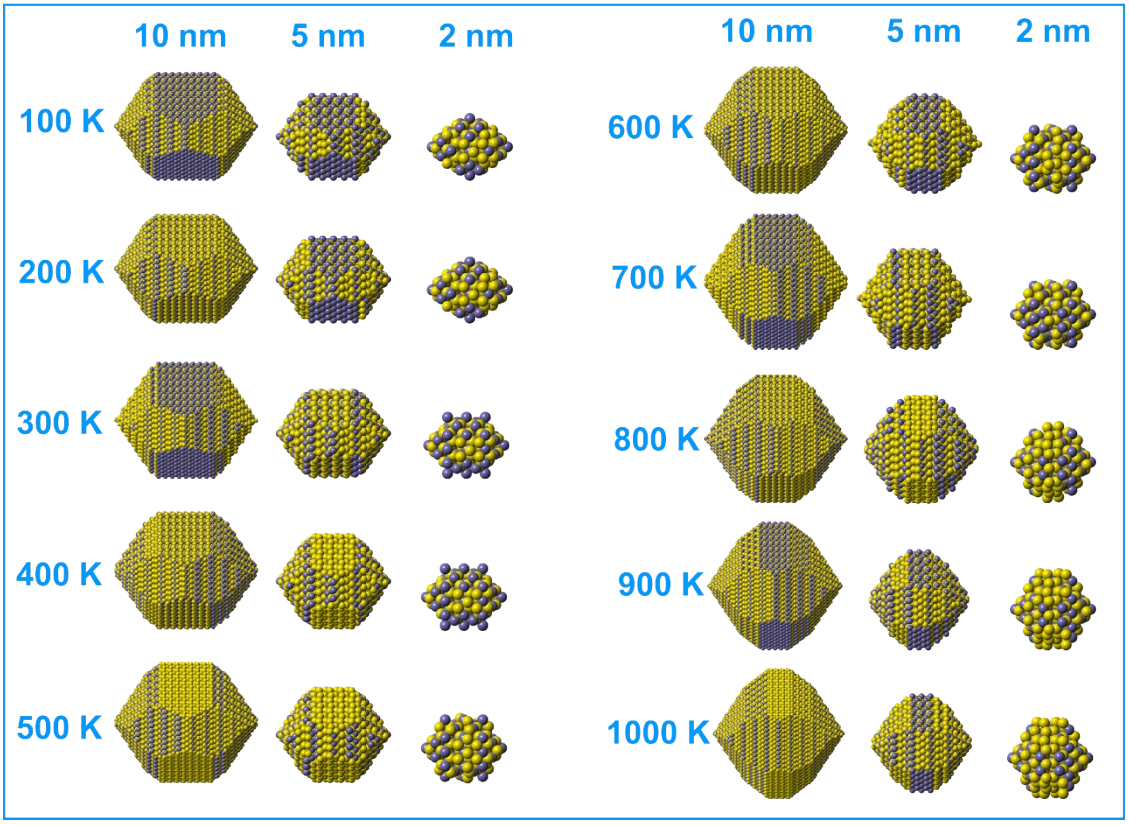

Fig. S20 The morphology of different size FeS_2-M nanoparticles under varying temperatures.

References

1 J. Liu, A. Xu, Y. Meng, Y. He, P. Ren, W. P. Guo, Q. Peng, Y. Yang, H. Jiao, Y. Li and X. D. Wen, *Comput. Mater. Sci.*, 2019, **164**, 99–107.

2 X.-W. Liu, S. Zhao, Y. Meng, Q. Peng, A. K. Dearden, C.-F. Huo, Y. Yang, Y.-W. Li and X.-D. Wen, *Sci. Rep.*, 2016, **6**, 1–10.

3 K. D. Kwon, K. Refson, S. Bone, R. Qiao, W. L. Yang, Z. Liu and G. Sposito, *Phys. Rev. B - Condens. Matter Mater. Phys.*, 2011, **83**, 64402.

4 M. Tokonami, K. Nishiguchi and N. Morimoto, *Am. Mineral.*, 1972, **57**, 1066–1080.

5 B. J. Skinner, R. C. Erd and F. Grimaldi, *Am. Mineral.*, 1964, **49**, 543–555.

6 S. L. Finklea, L. Cathey and E. L. Amma, *Acta Crystallogr. Sect. A*, 1976, **32**, 529–537.